

Numerical study of metastable states in Ising spin glasses

Andrea Cavagna, Irene Giardina and Giorgio Parisi

*Dipartimento di Fisica, Università di Roma “La Sapienza” and
Center for Statistical Mechanics and Complexity, INFM Roma 1,
Piazzale Aldo Moro 2, 00185 Roma, Italy*

(Dated: December 19, 2003)

We study numerically the structure of metastable states in the Sherrington-Kirkpatrick spin glass. We find that all non-paramagnetic stationary points of the free energy are organized into pairs, consisting in a minimum and a saddle of order one, which coalesce in the thermodynamic limit. Within the annealed approximation, the entropic contribution of these states, that is the complexity, is compatible with the supersymmetry-breaking calculation performed in [A.J. Bray and M.A. Moore, *J. Phys. C* **13** L469 (1980)]. This result indicates that the supersymmetry is spontaneously broken in the Sherrington-Kirkpatrick model.

In this last year there has been an outburst of new interest in the complexity of disordered systems, and in particular of spin-glasses [1, 2, 3, 4, 5, 6, 7, 8]. The complexity is the entropic contribution due to the exponentially large number of metastable states, and in mean-field disordered models it can be computed by calculating the number of minima of the Thouless-Anderson-Palmer (TAP) free energy [9]. Metastable states are crucial for the dynamical behaviour of disordered systems, and so is the complexity. Most notably, in glasses and some spin-glasses [10, 11] the complexity triggers a dynamical transition which is not associated to any static transition. Issues related to the analytic and numerical calculation of the complexity are therefore very relevant.

At the origin of the recent new studies there has been the observation done in [2], that the original calculation of the complexity for the Sherrington-Kirkpatrick (SK) model [12], performed by Bray and Moore in 1980 [13], breaks an intrinsic symmetry of the problem, namely a generalized form of the Becchi-Rouet-Stora-Tyutin (BRST) supersymmetry [14, 15]. Moreover, the supersymmetric complexity computed in [2] was found to be much smaller than the supersymmetry-breaking complexity of [13]. This discovery reopened, after more than twenty years, the problem of how to compute the complexity in the SK model, and, more in general, it raised the question of whether the BRST supersymmetry is spontaneously broken or not in disordered systems.

At the theoretical level, the situation is presently rather open. After the annealed calculation of [2], the supersymmetric (SS) complexity has been computed also at the quenched level [3, 4], showing that it is consistent with the static solution of the SK model and that it coincides with the one obtained from the Legendre transform method [16], at any level of replica symmetry breaking. However, it has been shown in [5, 6] that the SS complexity is stable only at the ground state free energy, where by definition it is zero. Thus, were the supersymmetry unbroken, this last result would lead to the conclusion that in the SK model the complexity of metastable states is in fact zero. On the other hand, the supersymmetry-

breaking (SSB) complexity (which has only been computed at the annealed level [13]) is non-zero and stable on a finite range of free energy densities. Moreover, it has recently been proved in [7] that the SSB complexity describes pairs of solutions of the TAP equations which are either minima or saddles of order one of the free energy. According to [7], the two solutions of each pair coalesce in the thermodynamic limit. In conclusion, the SS and SSB predictions differ considerably.

Given the ambiguous theoretical situation, a way to discriminate between the two pictures above, and thus to understand whether or not the BRST supersymmetry is spontaneously broken in the SK model, is to perform a numerical experiment. Of course, one may question what would be the dynamical role of the marginally unstable states described by the SSB complexity, but we do not deal with this problem in the present work. Our goal here is just to understand what is the structure of TAP solutions in the SK model, and which theoretical framework correctly describes this structure.

Our numerical results show that: i) all solutions of the TAP equations are either minima or saddles of order one of the free energy; ii) the solutions are organized into minimum-saddle pairs, connected along a mode which is softer the larger the system size; iii) the free-energy difference of the paired solutions decreases with increasing system size; iv) the annealed complexity of TAP solutions as a function of their free energy density is consistent with the SSB complexity of [13]. Our results therefore support the idea that the BRST supersymmetry is in fact broken in the SK model, and that the SSB complexity of [13] is correct within the annealed approximation.

The TAP equations for the SK model are,

$$\tanh^{-1} m_i + \beta^2 (1 - q) m_i - \beta \sum_j J_{ij} m_j = 0 , \quad (1)$$

where m_i are the local magnetizations, with $i = 1, \dots, N$, and the random couplings J_{ij} are drawn from a Gaussian distribution of mean zero and variance $1/N$. These equations are obtained by finding the stationary points of the

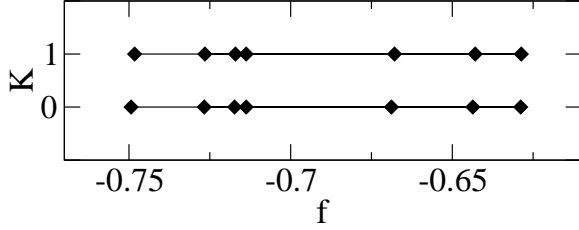


FIG. 1: Number of negative eigenvalues K vs free energy density f of 14 non-paramagnetic solutions of a sample at $N = 80$. The solutions are clearly paired into minimum-saddle couples, with very close value of f .

TAP free energy,

$$F_{TAP}(m) = -\frac{1}{2} \sum_{ij} J_{ij} m_i m_j - \frac{N}{\beta} \log 2 - \frac{N\beta}{4} (1 - q)^2 + \frac{1}{\beta} \sum_i \log(1 - m_i^2)/2 + m_i \tanh^{-1}(m_i) ,$$

where $q = (1/N) \sum_i m_i^2$ is the self-overlap of a solution. We solve numerically equations (1) by using the C routine BROYDN of Numerical Recipes [17] starting with random initial conditions. We analyze 20429 samples at $N = 20$, 5000 samples at $N = 30$, 1000 samples at $N = 40$, 347 samples at $N = 60$ and 77 samples at $N = 80$. All data are for $T = 0.2 T_c$. In order to make our search of solutions as exhaustive as possible, we use two methods. First, all solutions we find in a sample are found at least 5 times. Second, we monitor the Morse sum, $\sum_\alpha (-1)^{k_\alpha} = 1$, where k_α is the number of negative eigenvalues of solution α . For $N = 20, 30, 40, 60$ we discard samples where this identity is violated for more than ± 2 (the fraction of discarded samples is always lower than 1%). For $N = 80$, however, due to the low number of samples, we do not enforce this last check.

The first interesting result is that *all* solutions we find, at any value of N , are either minima, or saddles with one negative eigenvalue of the Hessian (the paramagnet is a minimum). As an example, the solutions of a sample at $N = 80$ are reported in Fig.1. Moreover, all non-paramagnetic solutions are organized into minimum-saddle pairs: by making a gradient descent starting from a saddle and moving along the negative mode, we reach in one direction a very close minimum [18], and in the opposite direction the paramagnetic state. Thus, TAP pairs are not directly connected to each other, but they are all connected to the central paramagnetic minimum in a star-like structure. The self-overlap q of a saddle is always smaller than that of the connected non-paramagnetic minimum. The important point is that the two solutions of each pair have very close free energy densities f : by plotting the average free energy density difference Δf as a function of N , we see that Δf decreases with N (Fig. 2). A power law fit of the data gives

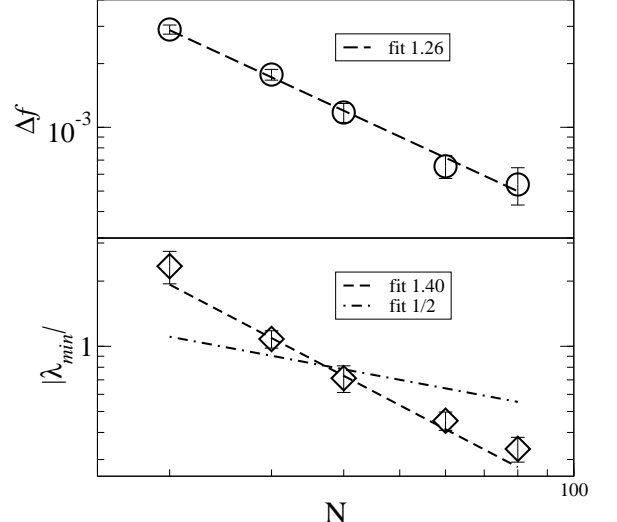


FIG. 2: Upper panel: the average free energy density barrier. Lower panel: the average modulus of the smallest eigenvalue. Lines are power law fits (see text).

$\Delta f \sim 1/N^{1.26}$. The paired solutions are connected along the saddle negative mode, which becomes the smallest positive mode of the nearby minimum. The fact that the two solutions have very close free energy suggests that this direction is extremely flat. In Fig.2 we also plot the average modulus of the smallest eigenvalue λ_{\min} as a function of N . A power law fit of the data gives $|\lambda_{\min}| \sim 1/N^{1.40}$. Thus the direction connecting the two solutions of a pair is flatter the larger N . The exponent 1/2 proposed in [7] seem to fit the data less satisfactorily.

These data suggests that for $N \rightarrow \infty$ the two solutions of each pair coalesce, forming a single, marginally unstable TAP solution. This conclusion is in qualitative agreement with the theoretical results of [7], results found in connection with the SSB annealed complexity. It is then natural to ask whether also the annealed numerical complexity is compatible with the SSB result of [13]. The annealed complexity is defined as,

$$\Sigma(f) = \frac{1}{N} \log \mathcal{N}(f) , \quad (2)$$

where $\mathcal{N}(f)$ is the number of solutions with free energy density f , averaged over the disorder J . The SSB annealed complexity is a smooth function of f , with a maximum at a free energy density f_{\max} . Let us define $\Sigma_{\max} = \Sigma(f_{\max})$ and $\Sigma''_{\max} = |\Sigma''(f_{\max})|$. For large N the *total* number of TAP solutions \mathcal{N} is given by,

$$\mathcal{N} = \int df e^{N\Sigma(f)} = e^{N\Sigma_{\max}} \sqrt{\frac{2\pi}{N\Sigma''_{\max}}} , \quad (3)$$

where we have expanded $\Sigma(f)$ to second order close to f_{\max} . The probability $p(f)$ of finding a solution with free

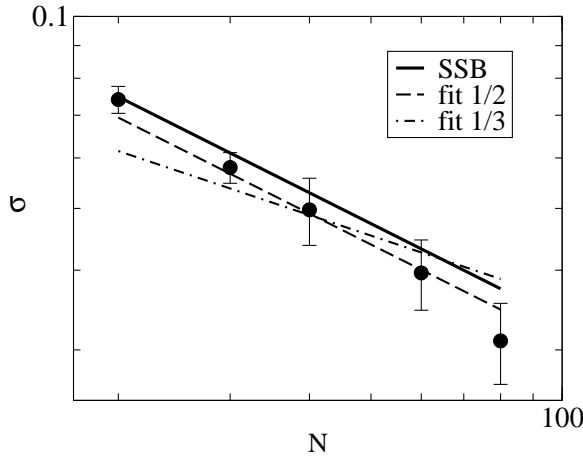


FIG. 3: The variance σ of the TAP solutions, an a function of N . Full line: the analytic prediction of the SSB calculation, $\sigma = 1/\sqrt{N\Sigma''_{\max}}$. Dashed line: best fit to $N^{-1/2}$. Dash-dotted line: best fit to $N^{-1/3}$.

energy density f is therefore given by,

$$p(f) = \frac{\mathcal{N}(f)}{\mathcal{N}} = \sqrt{\frac{N\Sigma''_{\max}}{2\pi}} e^{-\frac{1}{2}N\Sigma''_{\max}(f-f_{\max})^2},$$

which becomes a δ -distribution for $N \rightarrow \infty$. For finite N the probability distribution $p(f)$ is a numerically directly accessible quantity. In particular, its variance σ can be easily checked without the need of any binning of the data. In Fig.3 we plot the variance σ as a function of N . The full line is the prediction given by the SSB complexity, i.e. $\sigma = 1/\sqrt{N\Sigma''_{\max}}$, with $\Sigma''_{\max}^{(\text{SSB})} = 8.9$. Numerical data are compatible with the SSB prediction. Moreover, if we perform a fit to $\sigma \sim N^{-1/2}$ we find $\Sigma''_{\max} = 10.3$, and if we leave the exponent free, fitting to $\sigma \sim N^{-\gamma}$ we get $\gamma = 0.58$ (not shown). We also show the best fit to $\sigma \sim N^{-1/3}$, which is the exponent reported in [8]. This value, however, does not seem compatible with our data.

By making a (arbitrary) binning of the data in free energy, we can compute the full probability $p(f)$ and thus our numerical estimate of the complexity, $\Sigma(f) = \log[p(f)\mathcal{N}]/N$, where \mathcal{N} is the *total* average number of solutions per sample we find numerically. Results are shown in Fig.4 and compared to the theoretical curve of the SSB complexity $\Sigma(f)$. Even though the numerics is not excellent (especially for $N = 80$), the data seem compatible with the SSB prediction and clearly indicate that the annealed complexity is nonzero. However, a more quantitative comparison, not dependent on the binning, is clearly desirable. To do this we study the position of the maximum f_{\max} and the value of the complexity at this point Σ_{\max} , at various N . In order to avoid a measurement depending on the binning, we study the integral of $p(f)$, i.e. $g(f) = \int_0^f dx p(x)$, and interpolate $g(f)$ with a cubic function around its inflection point. In this way we have an estimate of both f_{\max}

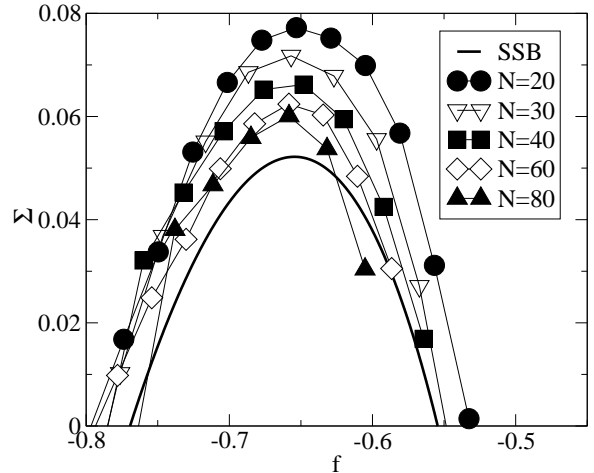


FIG. 4: Annealed complexity vs free energy density for various N ; lines connecting the points are only a guide for the eye. Full line: analytic SSB prediction.

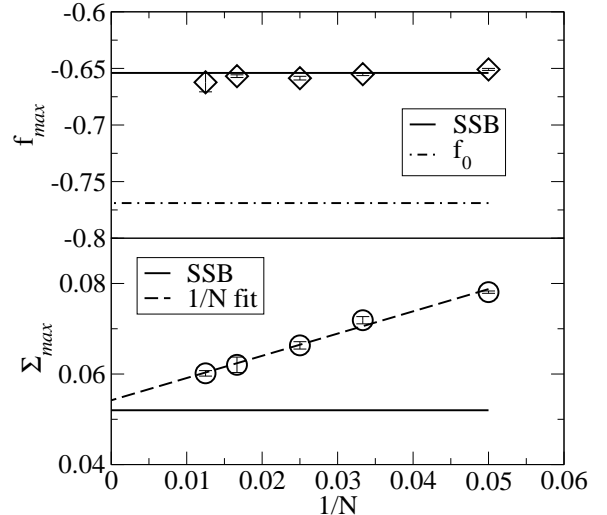


FIG. 5: Upper panel: f_{\max} as a function of $1/N$; the dash-dotted line is the value of the equilibrium free energy f_0 . Lower panel: Σ_{\max} , as a function of $1/N$; the dashed line is a $1/N$ fit to the data. In both panels, the full line is the $N = \infty$ value of the SSB prediction.

and Σ_{\max} , reported in Fig.5 as a function of $1/N$. The value of f_{\max} is basically constant, and it agrees quite well with the theoretical SSB value $f_{\max}^{(\text{SSB})} = -0.654$. On the same scale we report the value of the ground state (equilibrium) free energy density f_0 : our data do not seem compatible with the law $f_{\max} \rightarrow f_0$ for $N \rightarrow \infty$, proposed in [8]. The value of Σ_{\max} depends more strongly on N , as expected from equation (3), i.e. $\Sigma_{\max}^N = \Sigma_{\max}^{\infty} + \log(N\Sigma''_{\max})/(2N) + O(1/N)$. The extrapolation for $N \rightarrow \infty$ of our data for Σ_{\max} agrees very well with the SSB value $\Sigma_{\max}^{(\text{SSB})} = 0.052$.

A last important consistency check between our numerical data and the SSB calculation concerns the be-

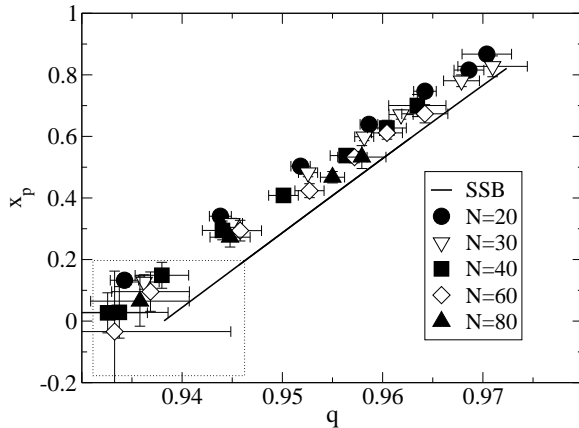


FIG. 6: The stability parameter x_p vs the self-overlap q , parametrically in the free energy density f . Full line: the analytic SSB prediction. Data in the box have $f < f_0$.

haviour of the overlap q and the stability parameter x_p , defined as, $x_p = 1 - \beta^2 \sum_i (1 - m_i^2)^2 / N$. In the thermodynamic limit the condition $x_p \geq 0$ must be satisfied in order to have a physically acceptable TAP state [19]. In fact, it is precisely this last condition which is violated by the SS complexity in all points but the equilibrium free energy f_0 . Both q and x_p depend on the free energy density f of the solutions. In Fig.6 we plot x_p as a function of q , parametrically in f , at various values of N . We see that x_p is in fact positive for all solutions in the region where $\Sigma(f) \geq 0$. The data agree quite well with the SSB prediction, even in the phase $f < f_0$, where $\Sigma(f) < 0$.

Our algorithm finds more easily solutions with lower free energy, as can be seen by checking the frequency each solution is found, and this effect is stronger the larger N . Therefore, at $N = 80$ (where the Morse check is not enforced) we are probably missing a number of solutions with $f > f_{\max}$. We believe this is the reason why the values of σ and f_{\max} at $N = 80$ in Figs. 3 and 5 are slightly smaller than expected, irrespective of error bars. The same problem arises in the reconstruction of $\Sigma(f; N = 80)$ for $f > f_{\max}$ in Fig.4. The problem of finding solutions at finite T of the TAP equations is well known, and for this reason numerical investigations in the past have been done by using alternative methods: $T = 0$ studies of one spin-flip stable states [20], naive TAP equations [21], or modified TAP equations [22]. To the best of our knowledge, the present work is the first extensive study of the full TAP equations at finite T .

In summary, our results support the conclusion that at the annealed level the complexity of the SK model is given by the SSB solution of [13], and therefore that the BRST supersymmetry is spontaneously broken in this system. Considering the fact that the supersymmetry is *not* broken in the p -spin spherical model, it may be argued that systems characterized by full replica symmetry breaking (as the SK model), and systems solved by one

step of replica symmetry breaking (as the p -spin), belong to two different classes also for what concerns the spontaneous breaking of the supersymmetry. The origin of this different behaviour must lie in the geometric structure of the states. In particular, the marginality of TAP saddle-minima pairs in the SK model is probably the cause of the spontaneous supersymmetry breaking. This fact is also likely to be connected to the different dynamical behaviour of these two classes of systems: the dynamics of the p -spin model is heavily influenced by the TAP states, while in the SK model, despite the non-zero SSB complexity, the dynamics asymptotically reproduces the static results, with no role played by the metastable states. The supersymmetry could then be an elegant way of distinguishing different dynamical classes.

We thank A. Bray, L. Leuzzi, M. Moore, T. Plefka, T. Rizzo and the Rome Complex Systems Group for discussions, and A. Annibale and E. Trevigne for the SSB data. We acknowledge support of the ESF-SPHINX program.

- [1] M. Mezard, G. Parisi, and R. Zecchina *Science* **297** 812 (2002).
- [2] A. Cavagna, I. Giardina, G. Parisi and M. Mezard *J. Phys. A* **36** 1175 (2003).
- [3] A. Annibale, A. Cavagna, I. Giardina and G. Parisi *Preprint* cond-mat/0307465 (2003).
- [4] A. Annibale, A. Cavagna, I. Giardina, G. Parisi and E. Trevigne *J. Phys. A* **36** 10937 (2003).
- [5] A. Crisanti, L. Leuzzi, G. Parisi, and T. Rizzo, *Preprint* cond-mat/0307082 (2003).
- [6] A. Crisanti, L. Leuzzi, G. Parisi, and T. Rizzo, *Preprint* cond-mat/0307543 (2003).
- [7] T. Aspelmeier, A. J. Bray, M. A. Moore *Preprint* cond-mat/0309113 (2003).
- [8] T. Plefka *Preprint* cond-mat/0310782 (2003).
- [9] D.J. Thouless, P.W. Anderson and R.G. Palmer *Phil. Mag.* **35** 593 (1977).
- [10] C.A. Angell, *J. Phys. Chem. Sol.* **49** 863 (1988).
- [11] A. Crisanti, H. Horner, and H.-J. Sommers, *Z. Phys. B* **92**, 257 (1993).
- [12] D. Sherrington and S. Kirkpatrick *Phys. Rev. Lett.* **32** 1792 (1975).
- [13] A.J. Bray and M.A. Moore *J. Phys. C* **13** L469 (1980).
- [14] C. Becchi, R. Rouet and A. Stora *Comm. Math. Phys.* **42** 127 (1975); I.V. Tyutin *Lebedev preprint* FIAN 39 (1975).
- [15] A. Cavagna, J.P. Garrahan and I. Giardina *J. Phys. A* **32** 711 (1998).
- [16] R. Monasson *Phys. Rev. Lett.* **75** 2847 (1995).
- [17] C.G. Broyden, *Math. Comp.* **19** 577 (1965).
- [18] The average distance is $d = [\sum_i (m_i^{(0)} - m_i^{(1)})^2 / N]^{1/2} \sim 0.1$, weakly dependent on N .
- [19] T. Plefka, *J. Phys. A* **15** 1971 (1982).
- [20] K. Nemoto, *J. Phys. A* **21** L287 (1988).
- [21] K. Nishimura, K. Nemoto and H. Takayama *J. Phys. A* **23** 5915 (1990).
- [22] T. Plefka, *Europhys. Lett.* **58** 892 (2002); T. Plefka *Phys. Rev. B* **65** 224206 (2002).